Work measurement in an optomechanical quantum heat engine

Ying Dong, Keye Zhang, Francesco Bariani, and Pierre Meystre

Phys. Rev. A **92**, 033854 — Published 28 September 2015

DOI: 10.1103/PhysRevA.92.033854

Work measurement in an optomechanical quantum heat engine

Ying Dong,[1,2] Keye Zhang,[3,1] Francesco Bariani,[1] and Pierre Meystre[1]

[1]*B2 Institute, Department of Physics and College of Optical Sciences, University of Arizona, Tucson, Arizona 85721, USA*
[2]*Department of Physics, Hangzhou Normal University, Hangzhou, Zhejiang 310036, China*
[3]*Quantum Institute for Light and Atoms, State Key Laboratory of Precision Spectroscopy, Department of Physics, East China Normal University, Shanghai, 200241, China*

We analyze theoretically measurement schemes of the mean output work and its fluctuations in a recently proposed optomechanical quantum heat engine [K. Zhang *et al.* Phys. Rev. Lett. **112**, 150602 (2014)]. After showing that this work can be operationally determined by continuous measurements of the intracavity photon number we discuss both dispersive and absorptive measurement schemes and analyze their back-action effects on the efficiency of the engine. Both measurements are found to reduce the efficiency of the engine, but their back-action is both qualitatively and quantitatively different. For dispersive measurements the efficiency decreases as a result of the mixing of photonic and phononic excitations, while for absorptive measurements, its reduction arises from photon losses due to the interaction with the quantum probe.

PACS numbers: 42.50.Wk, 07.10.Cm, 07.57.Kp

I. INTRODUCTION

The thermodynamic description of quantum heat engines (QHE), which has been discussed at least since the early days of laser physics [1], has recently attracted much interest [2–5], in part because the increased control achievable over microscopic and mesoscopic systems opens promising new avenues of theoretical and experimental investigation [6–11].

QHE can exhibit intriguing properties, including their potential to outperform their classical analogues. For example, it has been shown that a quantum photo-Carnot engine can extract work from a single reservoir if the latter has built-in quantum coherence [12], and its power can be increased by noise-induced coherence [13]. In a different situation, a trapped ion based quantum engine operating on an Otto cycle was shown theoretically to break the Carnot efficiency limit in the presence of a squeezed reservoir [10].

The definition of thermodynamical quantities in the quantum context presents however conceptual challenges [14–17], and much attention has been devoted to the proper definition and the quantum statistical properties of quantities such as heat, work and entropy [18–30]. In closed quantum systems work may be defined in terms of a two-time measurement scheme [31–34] or, in a recently proposed alternative approach, of a single projective measurement [35]. However the situation is less clear for open quantum systems, where there are still open questions regarding the definition and and experimental measurements of work and heat [31, 32, 36–38] due to the lack of energy conservation in the reservoir(s). In this context quantum stochastic thermodynamics [39, 40], like its classical counterpart [41], offers an interesting framework to discuss thermodynamic properties and simulate numerically the system behavior.

Optomechanical systems are prime candidates to investigate the properties of QHE. Thanks in particular to advances in nanofabrication they have witnessed rapid developments in the last decade and can now operate routinely deep in the quantum regime, with broad potential for applications in quantum technology [42]. Recently, three of us proposed and analyzed theoretically an optomechanical QHE based on an Otto cycle [43]. In this system the intracavity field of an optical resonator interacts coherently with a single mode of vibration of a mechanical element, for instance the center-of-mass motion of an oscillating end-mirror of a Fabry-Pérot resonator, via radiation pressure. In addition the optical field is incoherently coupled to a cold reservoir at $T \approx 0$ due to cavity losses, and the mechanics is likewise connected to a warmer thermal bath at the temperature of its substrate, for instance a mesoscopic solid state device. The control of the normal-mode dispersion of the coherently coupled phonon and photon modes (phonon polaritons) allows to cycle the system between the cold and warm temperature baths. This permits the realization of thermodynamical cycles via the manipulation of an external parameter such as the detuning between the driving optical field and the cavity resonance frequency. The exquisite experimental control that can be achieved in optomechanics suggests that such a QHE may be a good candidate to experimentally implement a measurement of the work output characteristics.

We consider this specific system to discuss several aspects of the work that can be extracted from QHE. Particular emphasis is placed on the development of operational approaches to the quantum measurement of the work and its fluctuations, and also on the back-action of these measurement on the efficiency of the system. (Measurement back-action on the quantum driving of quantum systems has recently been considered in Refs. [29, 30]).

We show that in the specific QHE under consideration work is performed on the mechanics by the radiation pressure of the intracavity photons responsible for the optomechanical coupling. That work can be evaluated from repeated measurements of the intracavity photon number, which is directly proportional to the radiation pressure force. We consider and contrast dispersive and absorptive continuous measurement schemes, both involving passing a stream of two-state atoms through the resonator. The former situation results in non-destructive measurements of the photon number, and the associated coupling between the normal modes of the optomechanical system, while the latter corresponds to the inclusion of an additional energy dissipation channel for the photons.

We numerically determine the mean work and its variance over the entire thermodynamical cycle for both measurement schemes and use these results to evaluate the measurement back-action in the thermodynamic cycle. Our analysis is carried out within the framework of quantum stochastic thermodynamics, with the measured work evaluated via continuous detection of the mean photon number in the cavity.

The paper is organized as follows. Section II briefly reviews the optomechanical QHE of Ref. [43] and the main features of the Otto cycle. In particular we draw attention to the fact that the two normal modes of the system undergo two distinct thermodynamic cycles. This will be important to keep in mind in the context of measurement back-action considerations. Section III defines the work output of the engine, using first the conceptually simpler case of classical measurements to show the relationship between the extracted work and the mean intracavity photon number. This result is used to justify an operational approach based on continuous measurements of the intracavity photon number operator to determine the expectation value of the quantum measurement of work and its fluctuations. Section IV introduces two such measurement schemes, which involve either the dispersive or the absorptive interaction between the cavity mode and a stream of two-state systems. Information on the intracavity field is then inferred from measurements of the state of the atoms after they exit the optomechanical resonator. Section V summarizes the results of numerical simulations obtained by a standard quantum trajectory approach to the solution of the stochastic Schrödinger equations describing the continuous measurements. Finally Section VI is a summary and outlook.

II. OPTOMECHANICAL OTTO CYCLE

This section briefly reviews the main features of the optomechanical quantum heat engine of Ref. [43]. We consider a standard optomechanical setup with a cavity mode of frequency ω_c and damping rate κ coupled via radiation pressure to a single oscillation mode of a mechanical resonator of frequency ω_m and damping rate γ. The cavity is driven by an optical pump field of amplitude $\alpha_{\rm in}$ and frequency ω_p. We assume that the system reaches a classical steady state with mean intracavity field amplitude $\alpha \approx \alpha_{\rm in}/\Delta$, where

$$|\Delta| = |\omega_p - \omega_c - 2\beta g| \gg \kappa \tag{1}$$

is the detuning between the pump and cavity fields corrected for the equilibrium position of the mechanical oscillator $\beta = -g\alpha^2/\omega_m$, and g is the single-photon optomechanical coupling constant.

Denoting the small fluctuations of the photon and phonon modes around the steady state (α, β) by the bosonic annihilation operators $\hat{a}$ and $\hat{b}$ respectively, the system is then described by the total Hamiltonian

$$\hat{H} = \hat{H}_{ab} + \hat{R}_\gamma + \hat{R}_\kappa + H_{\alpha\beta}. \tag{2}$$

Here

$$\hat{H}_{ab} = -\hbar\Delta\hat{a}^\dagger\hat{a} + \hbar\omega_m\hat{b}^\dagger\hat{b} + \hbar G(\hat{a}^\dagger + \hat{a})(\hat{b}^\dagger + \hat{b}), \tag{3}$$

is the linearized quantum optomechanical Hamiltonian [44], where we have introduced the linearized optomechanical coupling strength $G = \alpha g$. $\hat{R}_\gamma$ and $\hat{R}_\kappa$ account for the phonon and the photon dissipation into the hot and cold bath in the Otto cycle, respectively. Finally $H_{\alpha\beta}$ is the classical energy associated with the classical steady state (α, β).

We focus on the red detuned regime $\Delta < 0$, which in general leads to stable dynamics for small damping [42] and perform a Bogoliubov transformation to diagonalize the Hamiltonian (3) in terms of normal modes (polaritons) described by the bosonic annihilation operators $\hat{A}$ and $\hat{B}$. Ignoring a constant term that does not affect the dynamics this gives

$$\hat{H}_{AB} = \hbar\omega_A\hat{A}^\dagger\hat{A} + \hbar\omega_B\hat{B}^\dagger\hat{B}, \tag{4}$$

with normal mode eigenfrequencies

$$\omega_{A,B} = \sqrt{\frac{\Delta^2 + \omega_m^2 \pm \sqrt{(\Delta^2 - \omega_m^2) - 16G^2\Delta\omega_m}}{2}} \tag{5}$$

which are plotted in Fig. 1 as a function of the detuning Δ. It is straightforward to see that for $\Delta \ll -\omega_m$, the polariton "A" is photon-like and the polariton "B" is phonon-like, while in the opposite limit $-\omega_m \ll \Delta < 0$, it is the polariton "A" that is phonon-like and the polariton "B" is photon-like.

Consider then a situation where the phonon reservoir is at some finite temperature $T_{\rm phonon}$, while the optical field is coupled to a reservoir at $T = 0$ – an excellent approximation at visible frequencies – and concentrate first on the polariton "B" only. It is possible to realize an Otto cycle for that normal mode in the following way [45]: Start from the system in thermal equilibrium at a large negative detuning Δ, in which case "B" is essentially at the temperature of the phonon bath, with corresponding thermal excitation number $\langle\hat{B}^\dagger\hat{B}\rangle \equiv \bar{N}_B$, and adiabatically change Δ across the resonance $\Delta = -\omega_m$ in a time τ_1 to a small negative value close to 0 (but not too close to avoid the onset of instabilities). In that first adiabatic stroke the polariton "B" changes its character from phonon-like to photon-like, and the energy of the thermal phonons is converted into intracavity photons that perform work on the oscillating mirror via radiation pressure – more on that in the following section.

Once the detuning has reached its final value the system is allowed to thermalize with the cavity field reservoir at $T = 0$. This first thermalization stroke, of duration τ_2, releases heat in the process. The following stroke is again adiabatic (second adiabatic stroke). It consists in changing Δ back to its large negative value in a time τ_3. Finally the cycle is closed by allowing the polariton "B", which has now regained its phonon-like character, to thermalize with its reservoir at $T_{\rm phonon}$ by absorbing heat. This second thermalization stroke has a duration τ_4. The four strokes of the cycle are sketched schematically in Fig. 1(b).

The polariton "A" simultaneously also goes through a thermodynamic cycle, with however significant differences. First, it is initially coupled to a reservoir at $T \approx 0$, so that the initial thermal polariton occupation is $\langle\hat{A}^\dagger\hat{A}\rangle \equiv \bar{N}_A \approx 0$. Second, the first thermalization stroke for the "B" cycle, which takes a

time of the order of a few κ^{-1}, is not long enough to also thermalize the "A" polariton provided that the optical damping rate is much faster than the mechanical damping rate, $\kappa \gg \gamma$, which is normally the case in optomechanical systems. Under these conditions the population of mode "A" remains essentially unchanged and equal to zero, and the "A" cycle does not produce any work (positive or negative.) That is, provided that the changes in detuning Δ can be realized in a perfectly (quantum) adiabatic fashion, which includes but is not limited to avoiding the effects of dissipation, the two cycles remain completely decoupled. We can summarize these requirements via the set of conditions

$$1/\tau_4 < \gamma \ll 1/\tau_2 < \kappa < 1/\tau_{1,3} \ll G \ll \omega_m. \tag{6}$$

This, however, no longer holds if quantum adiabaticity is lost, for example as a consequence of a measurement process. This will have important consequences in the context of the dispersive quantum measurements of sections IV and V.

III. OUTPUT WORK

We now define the thermodynamical quantities that will be used in the following discussion. Cast in infinitesimal form, the first law of thermodynamics can be formally written as

$$dU = dW + dQ, \tag{7}$$

where U, Q, and W, are the internal energy, heat, and work, respectively. For a general open quantum system with density operator $\hat{\rho}$ and Hamiltonian $\hat{H}$ we have

$$U = \mathrm{Tr}[\hat{\rho}\hat{H}] \tag{8}$$

so that in the Schrödinger representation the average (classical) values of the infinitesimal work and heat increments are [4, 46]

$$dW = \mathrm{Tr}\left[\hat{\rho}(d\hat{H})\right], \tag{9}$$

$$dQ = \mathrm{Tr}\left[(d\hat{\rho})\hat{H}\right]. \tag{10}$$

As defined in Eq. (7) the work is positive for a positive change in the internal energy of the system. In the absence of heat exchange, for example during an adiabatic transformation, it corresponds to work performed on the system. We thus introduce also the output work performed by the system as its opposite,

$$W_{\mathrm{out}} \equiv -W, \tag{11}$$

This is the quantity that we use later to evaluate the efficiency of the QHE.

A. Output work in the optomechanical QHE

We have seen that in the normal mode picture the "B" polariton heat engine is driven through an Otto cycle. Provided

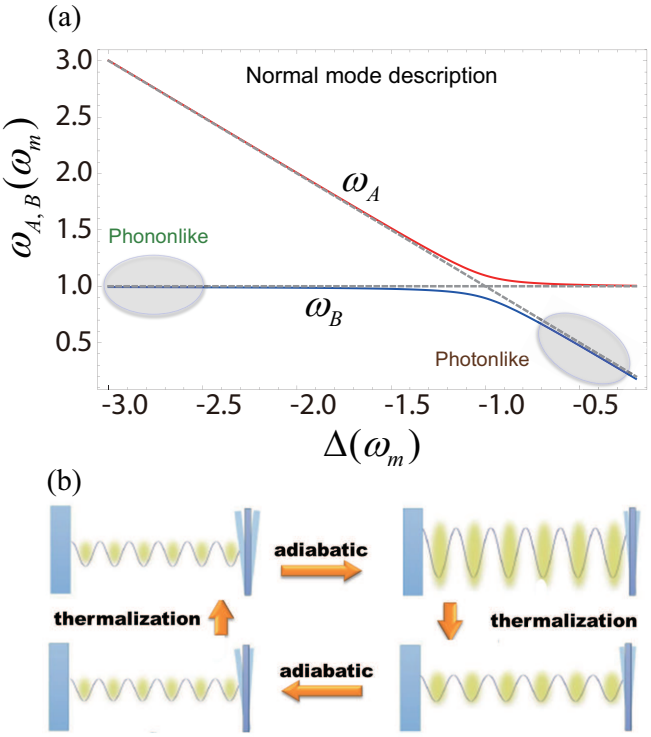

FIG. 1: (Color online) (a) Frequencies of the two normal modes (polaritons) of the optomechanical system for $G/\omega_m = 0.1$ in the red-detuned case $\Delta < 0$. The dashed lines correspond to the of the bare photon and phonon modes. The plot also illustrates that for large negative detunings the "B" polariton is phonon-like, and photon like for small negative detunings. (b) Intuitive physical picture of the Otto cycle. Initially (top left corner) the mechanics undergoes relatively large thermal fluctuations due to its coupling to a hot thermal reservoir. At the end of the first adiabatic step (top right corner), the polariton has however become photon-like. Its unchanged mean occupation, converted into photons, results in added radiation pressure force on the mechanics. Thermalization at rate κ to the temperature of the radiation reservoir $T \approx 0$ then significantly reduces the polariton occupation number (bottom right corner). At the end of the second adiabatic step, the polariton has regained its phononic nature, but now with small occupation number and hence a small adjustment of the mirror position (bottom left corner). Finally, the phonon-like polariton thermalizes to the temperature ot the hot phonon thermal bath in the final step, regaining the initial thermal occupation number at rate γ (back at top left corner).

that dissipation is weak enough to be negligible during the adiabatic strokes [see Eq. (6)], work is only performed by (or injected into) the system during those strokes, while heat is only exchanged during the thermalization steps [43]. Since the "B" polariton population is $\bar{N}_B = 0$ after thermalization with the optical heat bath at $T = 0$ we can then restrict the determination of the work to the first adiabatic stroke, where

$$dQ = \mathrm{Tr}[(d\hat{\rho}_{AB})\hat{H}_{AB}] = 0, \tag{12}$$

and

$$dW = \mathrm{Tr}[\hat{\rho}_{AB}(d\hat{H}_{AB})] = \bar{N}_B \hbar d\omega_B. \tag{13}$$

Here we have used the normal mode picture of the Hamiltonian (4) and taken $\bar{N}_A \approx 0$, as previously discussed. Since in the adiabatic stroke $\bar{N}_B$ is conserved, the average work is simply given by the change in energy of mode "B",

$$W = \int_{\Delta_i}^{\Delta_f} dW = \hbar[\omega_B(\Delta_f) - \omega_B(\Delta_i)]\bar{N}_B, \tag{14}$$

where Δ_i and Δ_f are the initial and final detunings, see Eqs. (1) and (5). Note also that in the case of perfect adiabaticity, the "B" polariton number distribution gives directly the full statistical distribution of the work as well.

Alternatively one can also work in the bare modes representation, where the photon and phonon distributions are time dependent. Equation (9) then takes the form

$$dW = \mathrm{Tr}[\hat{\rho}_{ab}(d\hat{H}_{ab})] = -\hbar\bar{n}_a d\Delta, \tag{15}$$

where we have used the fact that the only term in Hamiltonian (3) with a Δ dependence is the free field part $-\hbar\Delta\hat{a}^\dagger\hat{a}$, and $\bar{n}_a = \langle\hat{a}^\dagger\hat{a}\rangle$ is the average number of excitations in the photon mode $\hat{a}$. In this picture the average work is given by

$$W = -\hbar\int_{\Delta_i}^{\Delta_f} \bar{n}_a(\Delta)d\Delta. \tag{16}$$

If the stroke is perfectly adiabatic the values of the average work obtained from expressions (14) and (16) are equal. However if either the optical or the mechanical damping is significant on the time scale of the adiabatic stroke, or if the variation of the optical detuning induces non-adiabatic transitions and in particular a non-vanishing population of polariton $\hat{A}$, then Eq. (14) is no longer exact. The expression of the average work (16) in terms of the mean photon number remains however valid, as confirmed by a classical analysis to which we now turn.

IV. QHE WORK MEASUREMENT

We now discuss several possible measurement schemes that can be considered to quantify the work performed by the heat engine and its fluctuations and that are experimentally realizable in principle. To set the stage we first consider a simple classical approach before considering two types of quantum measurements.

A. Classical measurement scheme

A simple way to implement the variation in detuning $\Delta(t)$ required for the adiabatic strokes of the QHE is through a change in cavity length,

$$\Delta(t) \to \Delta(y) = \Delta_0 - g_M y. \tag{17}$$

Here y is a *classically* controlled length change, assumed small compared to the total cavity length, $g_M \equiv g/y_M$ is the optomechanical coupling normalized to the mirror zero-point motion y_M , and Δ_0 is a nominal detuning. We can then express W in terms of the spatial integral of the position-dependent radiation pressure force $F_{\mathrm{rp}}(y)$ as

$$W = \int_{y_i}^{y_f} F_{\mathrm{rp}}(y)dy \tag{18}$$

where

$$F_{\mathrm{rp}}(y) = \hbar g_M \bar{n}_a(y). \tag{19}$$

A possible classical scheme to measure the work output of the engine is illustrated in Fig. 2. The optomechanical resonator comprises the oscillating end mirror driven by radiation pressure and an *input* mirror of large mass M whose *classical* position y is controlled externally by the potential $V(y)$ provided by a piezoelectric element, thereby controlling the detuning $\Delta(y)$ in the presence of the radiation force F_{rp}. To use a thermodynamical metaphor, we may think of the input mirror as a classical piston that is pushed by the expanding photon gas.

Neglecting dissipation, the total system Hamiltonian is then

$$\hat{H}_m = \hat{H}_{ab} + H_M, \tag{20}$$

where $\hat{H}_{ab}$ is given by Eq. (3) with $\Delta = \Delta(y)$, and

$$H_M = \frac{p^2}{2M} + V(y) \tag{21}$$

is the classical Hamiltonian for the massive control mirror. The classical equations of motion for that mirror are then

$$\frac{dy}{dt} = \frac{\partial H_m}{\partial p} = \frac{p}{M}, \tag{22}$$

$$\frac{dp}{dt} = -\frac{\partial H_m}{\partial y} = -\frac{\partial V(y)}{\partial y} - F_{\mathrm{rp}}, \tag{23}$$

where H_m is the classical limit of the measurement Hamiltonian $\hat{H}_m$. If M is large enough that it can be considered as essentially infinite compared to all other optomechanical elements we have $dy/dt \approx dp/dt \approx 0$. That is, the force exerted by the control system balances the expectation value of the radiation pressure force,

$$-\frac{\partial V(y)}{\partial y} = F_{\mathrm{rp}}. \tag{24}$$

This shows that provided the kinetic energy of the large mirror remains essentially zero, all work performed by the photons is converted to the control potential energy and can be measured in that way. This confirms the intuitive result that the measurement of the work can be performed by sensing the radiation pressure force, proportional to the mean number of intracavity photons.

B. Continuous quantum measurements

We now turn to the measurement of the work in the quantum regime. For an isolated quantum system it can be determined unambiguously via a two-time measurement process [31, 32], but this approach is problematic for open quantum systems since it would require additional measurements

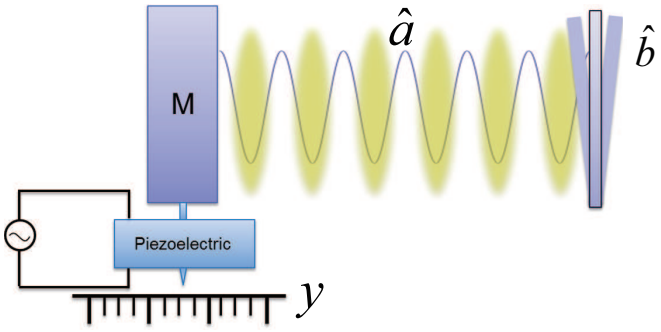

FIG. 2: (Color online) Schematic setup for a classical measurement of the output work, whereby the work performed by radiation pressure acting on the mirror of large mass M can be stored in the control system. See text for details.

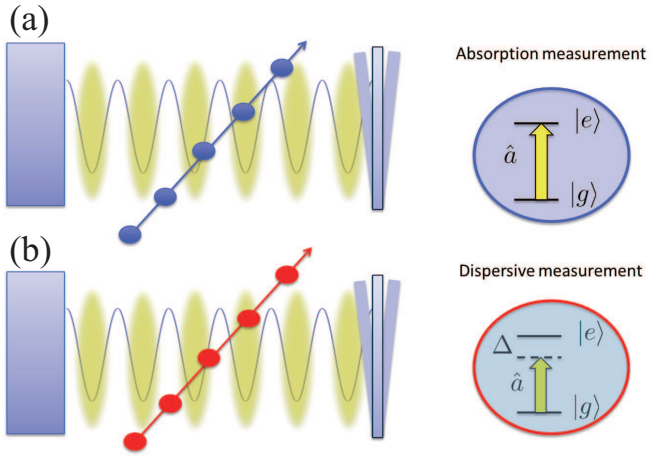

FIG. 3: (Color online) Schematic setup for a continuous quantum measurement of the output work with a beam of two-level atoms. a) Absorptive measurement: the cavity field is resonant with the atomic transition and the coupling induces real oscillations in the atomic population, which result in the loss of intracavity photons. b) Dispersive measurement: the cavity mode frequency is far off-resonant from the two-level atom transition frequency, resulting in a dispersive interaction that only modifies the phase of the atomic ground state wave function. See text for details.

on the reservoirs. In order to circumvent this issue, we adopt in the following an experimentally realizable operational approach based on stochastic quantum thermodynamics [39].

It is not possible to directly monitor the occupation of the polariton mode "B" since it consists of quasiparticles that are coherent superpositions of photon and phonon states. What is readily experimentally accessible is the intracavity optical field. Building on the discussion of the classical measurement scheme of the previous section our approach involves therefore weak continuous measurements [47] that monitor the intracavity photon number. We then calculate the total work by performing the integral in Eq. (16).

To this end we add to the Hamiltonian the interaction $\hat{V}_a$ between the system and the quantum probes used to extract information on its state, as well as a term $\hat{R}_a$ that accounts for the additional dissipative effects associated with these probes. The Hamiltonian (2) becomes then

$$\hat{H}_m = \hat{H} + \hat{V}_a + \hat{R}_a, \tag{25}$$

We consider specifically continuous measurements realized by passing through the resonator a dilute beam of two-level atoms that interact weakly with the intracavity field mode either resonantly or dispersively, with at most one atom at a time inside the resonator. The state of the field is inferred from a projective measurement on the atoms after they exit the cavity. We study both the cases of absorptive and dispersive atom-field interactions, see Fig. 3. Since $\hat{V}_a$ does not commute with the optomechanical Hamiltonian $\hat{H}_{ab}$ the measurements lead in general to a back-action on the QHE that affects both its output work and its efficiency.

In the following we use a quantum trajectory method to simulate quantum measurement processes and investigate their influence on the mean work W and its fluctuations ΔW^2. Our starting point is the description of the dynamics of open quantum systems in terms of a large ensemble of N quantum trajectories $\{|\psi_j(t)\rangle\}$ that are solutions of a stochastic Schrödinger equation of the general form

$$d|\psi(t)\rangle = (\mathcal{D}dt + \mathcal{R}dw)|\psi(t)\rangle. \tag{26}$$

The superoperator $\mathcal{D}dt$ accounts for both the Hamiltonian evolution of the system and non-unitary contributions that include dissipation and decoherence mechanisms associated with measurement processes, while the stochastic term $\mathcal{R}dw$, where dw describes one or more Wiener processes of zero mean with $dw^2 = dt$, accounts for the stochastic quantum jumps resulting from both reservoir noise and quantum measurements [48–50]. The initial conditions $|\psi_j(0)\rangle$ are selected consistently with the initial thermal distribution characterizing the density operator of the system. For completeness the main steps in the derivation of the stochastic Schrödinger equation for continuous measurements are briefly outlined in an Appendix.

1. *Absorptive measurements*

Consider first the resonant situation where a low density beam of probe two-state systems of transition frequency $\omega_{eg} = \omega_c$, and prepared in their ground state $|g\rangle$ is injected inside the optical cavity, see Fig. 3(a). The atom-field coupling is given in the rotating wave approximation by

$$\hat{V}_a = \hbar g_a(\hat{a}^\dagger \hat{\sigma}_{ge} + \hat{a}\hat{\sigma}_{eg}) \tag{27}$$

where g_a is the single-photon Rabi frequency of the transition and $\hat{\sigma}_{ij} = |i\rangle\langle j|$. For each quantum trajectory j, the effect of the continuous measurements is described by the stochastic Schrödinger equation [47, 51]

$$\begin{aligned} d|\psi_j(t)\rangle \;=\; & \left\{\left[-\frac{i}{\hbar}\hat{H}_{ab} - \frac{1}{2}\lambda_a\left(\hat{a}^\dagger\hat{a} - \langle\hat{a}+\hat{a}^\dagger\rangle\hat{a} + \frac{\langle\hat{a}+\hat{a}^\dagger\rangle^2}{4}\right)\right]dt \right. \\ & \left. + \sqrt{\lambda_a}\left(\hat{a} - \frac{\langle\hat{a}+\hat{a}^\dagger\rangle}{2}\right)dw\right\}|\psi_j(t)\rangle, \end{aligned} \tag{28}$$

where dw is a Wiener process,

$$\lambda_a = g_a^2 \tau \tag{29}$$

is a measure of the strength of the measurement, and τ is the transit time of an individual atom through the resonator. Note that in obtaining Eq. (28) the time increment dt is assumed to be long compared to the atomic transit time τ, so that this equation describes the statistical effect on the field of a large number of atomic measurements.

The term proportional to λ_a on the right-hand side of Eq. (28) accounts for the additional dissipation channel of the intracavity field resulting from the absorption of photons by the successive atoms, and the term proportional to $\sqrt{\lambda_a}$ describes the stochastic changes of the intracavity field about its expected value $\langle \hat{a} + \hat{a}^\dagger \rangle$ resulting from the stochastic measurement outcomes.

2. Dispersive measurements

We now turn to the situation where the interaction between the two-level atoms and the intracavity field mode is off-resonant. Upon adiabatic elimination of the upper electronic state, it is described by the effective Hamiltonian

$$\hat{V}_a = \hbar g_d \hat{a}^\dagger \hat{a} (\hat{\sigma}_{ee} - \hat{\sigma}_{gg}) = \hbar g_d \hat{a}^\dagger \hat{a} (\hat{\sigma}_{+-} + \hat{\sigma}_{-+}), \tag{30}$$

where $|\pm\rangle = (|e\rangle \pm |g\rangle)/\sqrt{2}$, and $g_d = g_a^2/2\delta$ is the off-resonant effective Rabi frequency coupling between the atoms and the intracavity intensity, with $\delta = \omega_c - \omega_{eg}$.

The atoms are now prepared in the superposition $|+\rangle$ of the ground and excited states, and information on the intracavity field is inferred from a change in phase of the atomic state. In that situation the effect of the measurements on the optical field is described by the stochastic Schrödinger equation [52]

$$\begin{aligned} d|\psi\rangle \;=\; & \left\{ \left[-\frac{i}{\hbar} \hat{H}_{ab} - \frac{1}{2} \lambda_d \left(\hat{n}_a - \langle \hat{n}_a \rangle \right)^2 \right] dt \right. \\ & \left. +\; \sqrt{\lambda_d} (\hat{n}_a - \langle \hat{n}_a \rangle) dw \right\} |\psi(t)\rangle, \end{aligned} \tag{31}$$

where $\lambda_d = g_d^2 \tau$.

As was the case for resonant coupling this equation also comprises two contributions, the second one accounting for the stochastic changes of the mean intracavity intensity $\langle \hat{n} \rangle$ about its expected value resulting from successive measurements. But because of the quantum non-demolition nature of the non-resonant atom-field interaction for the mean photon number $\langle \hat{a}^\dagger \hat{a} \rangle$, the dissipative channel of Eq. (31) is now replaced by a number conserving term that results in additional damping of the phase of the optical field.

Importantly, for the specific QHE considered here the effective interaction (30) couples the polariton branches "A" and "B" and transfers excitations between them. As we see in section V the result of these transitions is similar to that of nonadiabatic coupling. It has in general a significant impact on the work that can be extracted in the Otto cycle of the "B" polariton [43]. This is in contrast to absorptive measurements, in which case the interaction (27) does not significantly couple the two normal modes. Still, both measurement schemes result in the appearance of additional photon loss channels that limit the amount of extractable work. In both cases these measurement back-action mechanisms may be viewed as heat exchange between the engine and the environment.

3. Statistics of work from quantum trajectories

Solving the stochastic Schrödinger equations (28) and (31) repeatedly generates a set of trajectories $|\psi_j(t)\rangle$ that can be used to evaluate the statistics of any field observable. For each trajectory we can use this information to operationally define a stochastic variable associated with the work along that specific quantum trajectory for the time interval t_i to t_f as [39, 53]

$$W_j = \mathrm{Tr}[\hat{\rho}_j \hat{H}_{ab}(t_f)] - \mathrm{Tr}[\hat{\rho}_j \hat{H}_{ab}(t_i)] - \int_{t_i}^{t_f} \mathrm{Tr}[(\partial_t \hat{\rho}_j) \hat{H}_{ab}(t)] dt \tag{32}$$

where $\hat{\rho}_j(t) = |\psi_j(t)\rangle\langle\psi_j(t)|$ is the stochastic density operator associated with the j^{th} trajectory.

The difference between the first and second terms on the right side of this equation gives the internal energy difference, and according to Eq. (10), we identify the third term as the heat exchanged with the reservoirs along the trajectory. In terms of the stochastic states $|\psi_j\rangle$ used instead of $\hat{\rho}_j(t)$ to limit the memory requirements of the numerics W_j reads

$$W_j = \int_{t_i}^{t_f} \langle \psi_j(t) | \frac{\partial \hat{H}_{ab}}{\partial t} | \psi_j(t) \rangle dt, \tag{33}$$

a form consistent with Eqs. (9) and (16). While admittedly failing to answer fundamental open questions about the definition of work in open quantum systems, operationally this is how an experimentalist would extract the work performed by radiation pressure on the QHE.

The average and the variance of the work are then obtained as the first and second moments of this distribution as

$$W \equiv \sum_{j=1}^{N} \frac{W_j}{N}, \tag{34}$$

and

$$\Delta W^2 \equiv \sum_{j=1}^{N} \frac{(W_j - W)^2}{N}. \tag{35}$$

In the limit $N \to \infty$, the statistics resulting from the quantum trajectories approach the correct result. The numerical simulations presented in section V are based on this approach.

V. NUMERICAL RESULTS

This section presents selected results from numerical simulations of the continuous measurement of the work output of the QHE and its fluctuations as defined in equations (34) and

(35), both for absorptive and dispersive measurements. The numerical results were obtained by averaging for each choice of parameters 20,000 trajectories obtained from the stochastic Schrödinger equations (28) and (31) .

As mentioned above, to guarantee that the adiabatic strokes are indeed adiabatic in the absence of measurements, it is important to change $\Delta(t)$ sufficiently slowly that non-adiabatic transitions between the two polariton branches remain negligible, but fast enough that the damping of both the optical field and the mechanical oscillator at rates κ and γ respectively, remain negligible. This is particularly the case near the avoided crossing at $\Delta = -\omega_m$. The inset of Fig. 4 shows as an example the time evolution of $\Delta(t)$ (in units of ω_m) used in the simulations of the first adiabatic stroke to minimize this problem, with $\Delta(t)$ changing rapidly away from the avoided crossing and very slowly in its vicinity. As a result non-adiabatic transitions remain negligible, as illustrated in the black curves (labeled by a square) of Fig. 4. The population of the "B" polariton mode remains essentially constant during the adiabatic stroke, and the "A" polariton population remains essentially zero.

The additional curves in Fig. 4 show the time dependence of the average populations $\bar{N}_A(t)$ and $\bar{N}_B(t)$ during the first stroke of the heat engine, again neglecting mechanical and optical damping, for both dispersive (red lines with triangles) and absorptive (blue lines with circles) measurements. (Note that in the latter case $\bar{N}_A$ remains extremely small during that stroke and its evolution is nearly indistinguishable from the situation without measurements.) This is the most important stroke as far as extracting work from the engine is concerned, since the population of normal mode "B" remains extremely small during the second adiabatic stroke as a result of its thermalization at the optical reservoir temperature $T = 0$. In these examples the temperature $T_{\rm phonon}$ of the phonon bath and the initial detuning $\Delta(0)$ are chosen such that $\bar{N}_B(0) \approx 4$ and $\bar{N}_A(0) \approx 0$.

Comparing the evolution of the mean populations of the polariton modes for absorptive and dispersive measurements illustrates clearly the difference in their back-action on the operation of the QHE. In the case of absorptive measurements the "B" polariton population decreases significantly during what would otherwise be an adiabatic, population-conserving stroke. Since that stroke occurs fast compared to κ^{-1}, the observed damping results solely from an additional photon dissipation at rate λ_a due to the measurements, see Eq. (28). Importantly, though, these measurements do not result in any significant transfer of population to the "A" polariton.

The situation is qualitatively quite different for dispersive measurements. In that case there is no significant loss in total polariton population, but instead a significant transfer of population from mode "B" to mode "A". This is because the effect of dispersive measurements is an additional source of decoherence, but no loss of population, see Eq. (31). Dispersive measurements change the frequency of the photons stochastically, as seen by the term proportional to $\hat{a}^\dagger\hat{a}$ in (31), and thereby they change the structure of the polaritons. In contrast, in the absorptive case the measurements remove excitations from the system, but without affecting the structure

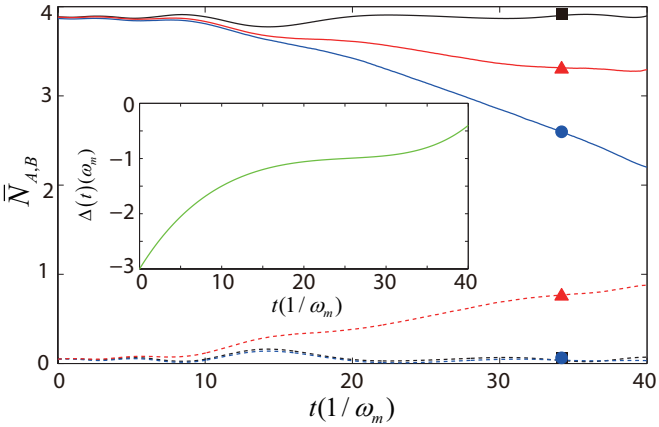

FIG. 4: (Color online) Time evolution of the mean excitations $\bar{N}_B$ and $\bar{N}_A$ of the polariton modes "B" (solid lines) and "A" (dashed lines) during the first stroke of the heat engine, averaged over 20,000 trajectories of the stochastic Schrödinger equation. Black lines marked by squares: no measurement. Red lines marked by triangles: Dispersive measurement with $\lambda_d = 0.04\omega_m$. Blue lines with circles: absorptive measurements with $\lambda_a = 0.04\omega_m$. Other parameters: $G = 0.2\omega_m$, $\Delta_i = -3\omega_m$, $\Delta_f = -0.4\omega_m$,$\kappa = 5\times10^{-3}\omega_m$ and $\gamma = 10^{-4}\omega_m$. Inset: time dependence of the pump-cavity detuning $\Delta(t)$ in units of ω_m. Time in units of $1/\omega_m$.

of the polaritons.

The population transfer between the normal modes "B" and "A" associated with dispersive measurements causes a reduction in the work performed by the system that can become quite dramatic due to the resulting unavoidable coupling between the two normal modes. Since for the polariton branch "A" the Otto cycle is reversed and produces negative *output* work [43], that is, work is performed by the environment on the polariton [54], one can even reach situations where the effective available work of the two systems, which are inextricably coupled, becomes negative. For absorptive measurement, in contrast, the two normal modes remain essentially uncoupled, and although the output work can be significantly reduced it always remains positive.

Figure 5(a) shows the mean value of the output work $W_{\rm out}$ for increasing measurement strength $\lambda_{a,d}$, illustrating its reduction due to measurement back-action. Surprisingly perhaps for equal measurement strengths dispersive measurements cause a stronger reduction in work than absorptive measurements. Since the thermalization processes are not affected by the measurement scheme the heat absorbed by the system from the mechanical reservoir, $Q_{\rm in}$, remains the same for all scenarios. For this reason, the efficiency of the quantum heat engine follows directly from the work as

$$\eta = \frac{W_{\rm out}}{Q_{\rm in}}. \tag{36}$$

We now turn to the fluctuations of the output work. Their variance, plotted in Fig. 5(b), shows a significant quantitative difference between the situations for absorptive and dispersive measurements. In the first case (dotted line) the fluctuations decrease monotonically as a function of the measure-

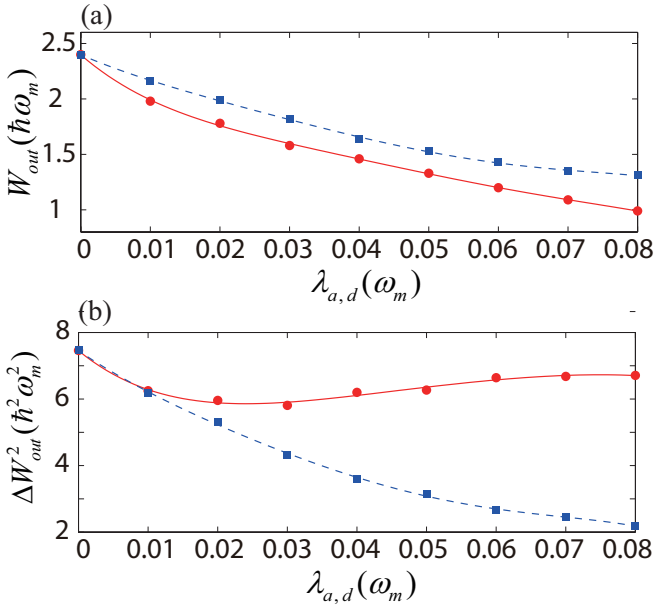

FIG. 5: (Color online) (a) Expectation value and (b) variance of the output work , in units of $\hbar\omega_m$, for the full cycle as a function of the measurement strength $\lambda_{a,d}$ (in units of ω_m). The points are results of numerical simulations and the lines serve to guide the eye. In both figures, the squares (red solid line) and circles (blue dashed line) stand for the dispersive and absorptive measurement scheme respectively. The statistic is performed upon 20000 trajectories. The stroke times are $\tau_1 = 40\omega_m^{-1}$, $\tau_2 = 400\omega_m^{-1}$, $\tau_3 = 40\omega_m^{-1}$, $\tau_4 = 4\times 10^4\omega_m^{-1}$. All other parameters as in Fig. 4.

ment strength, while in the case of dispersive measurements they remain roughly constant.

One can gain a better understanding of this behavior from the probability distribution $P(W_{j,\mathrm{out}})$ of the output work as a function of measurement strength. Figure 6 shows this distributions in the absence of measurements and for two measurement strengths, for both dispersive and absorptive measurements. Without measurements the probability distribution consists of a series of discrete peaks that correspond to the distribution of Fock states in the initial thermal distribution of the mechanical oscillator. Assuming perfect adiabaticity each of these mechanical Fock states is converted into a photonic Fock state during the first adiabatic stroke, and produces a specific amount of work. (The width of the peaks is due to residual non-adiabatic effects.)

Continuous measurements result in a broadening of the peaks, an effect of the stochastic nature of the detection process (see upper panels of Fig. 6) and, in the case of absorptive measurements, a decrease in amplitude of all peaks except the one corresponding to the vacuum field, a consequence of the additional photon decay channel. This is the reason for the reduction in variance as the measurement strength is increased. In contrast, for dispersive measurements the distribution shifts toward negative values of the work. This is more apparent in the lower panels, which show the same distribution on a logarithmic scale. This is a direct consequence of the coupling with the "A"-polariton engine cycle which, as we have seen, tends to be characterized by negative work. Because absorptive measurements don't couple the polariton modes in any significant way, this effect is almost completely absent in that case. Finally, since the mean total number of polaritons in modes "A" and "B" varies slightly over the chosen measurement strengths, the changes in the photon distribution are much less significant than for absorptive measurements, resulting in weak changes in the variance of the extracted work as a function of measurement strength.

VI. SUMMARY AND OUTLOOK

Summarizing, we have developed a measurement model to characterize the mean work and its fluctuations in an optomechanical QHE and performed a numerical study of the effect of continuous quantum measurements on its performance. We considered measurement schemes involving the continuous monitoring of the intracavity photon field, with both dispersive and absorptive interactions with a dilute beam of two-level atoms. By determining the average value and the variance of the work we are able to quantify the measurement back-action effects. In both cases, the measurements were found to induce a reduction in the average work performed by the engine and thus a reduction in its efficiency. However, the detailed reasons behind these reductions are qualitatively different. In the dispersive regime, the measurement induces transitions between the two polariton modes, and hence two thermodynamic cycles, one producing negative and the other positive work. The final result is a reduction of the efficiency with increased fluctuations in the work output. In the absorptive detection scenario, in contrast, photons are lost from the system via the interaction with the quantum probe that acts as an effective (zero temperature) reservoir. In this case, both the average value and the fluctuations of the work decay monotonically.

Because the nature of the photon-phonon polaritons can easily be changed, and in addition the photon and phonon modes are coupled to thermal reservoirs at different temperatures, one can use related ideas to develop additional thermodynamic applications of quantum optomechanical systems. One such example is a heat pump that uses a polariton fluid to cool additional phonon modes of frequencies not limited by the cavity-optical field detuning deep into the quantum regime from room temperature. The difference with more conventional heat pumps is that instead of moving a cooling fluid spatially trough expansion and compression cycles it is controlled by the polariton dispersion relation, changing the polariton fluid from photon-like to phonon-like, with the heat exchange between the mode to be cooled and the fluid achieved by phonon population transfer, and heat disposal achieved by coupling the photon-like polariton fluid to its thermal reservoir at T $\approx$ 0. This, and other possibilities, will be considered in future work.[55]

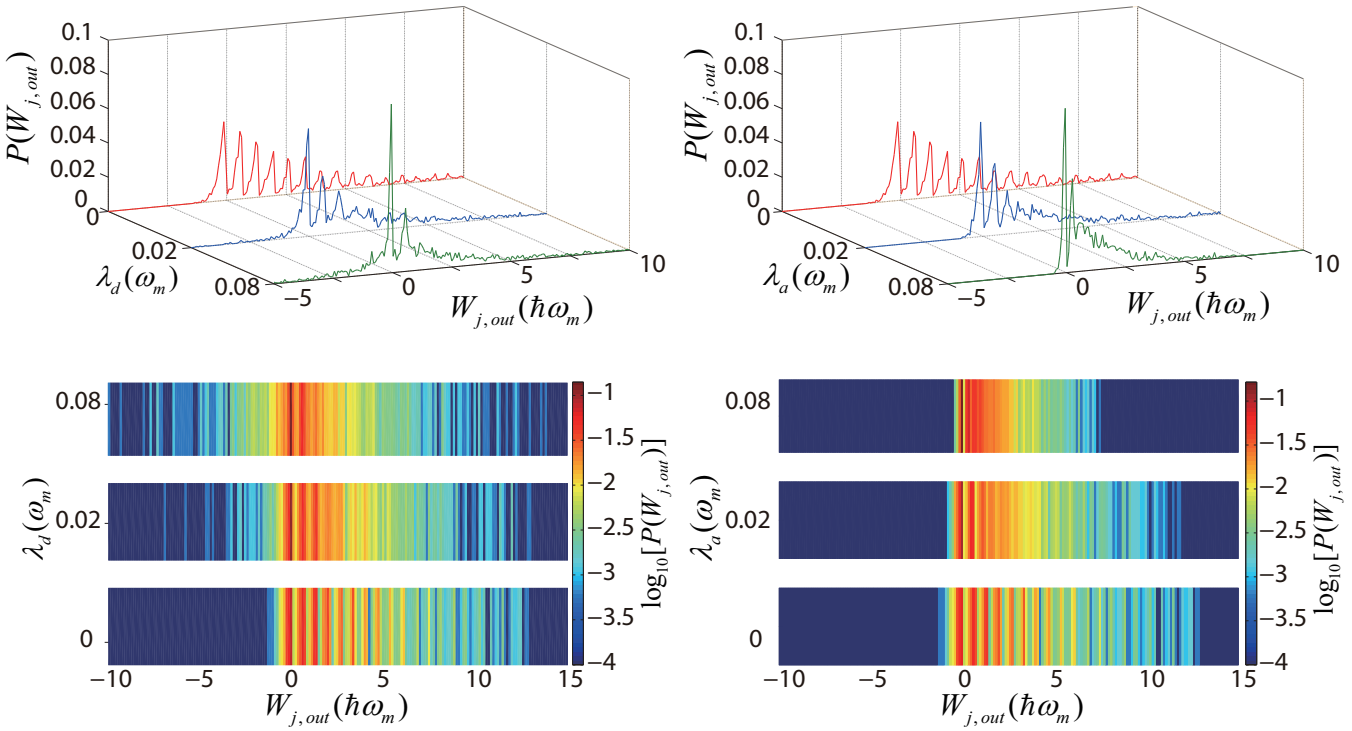

FIG. 6: Linear (upper panel) and logarithmic (lower panel) plots of the probability distribution of the output work, $W_{\rm out}$ (in units of ω_m) for dispersive (left column) and absorptive(right column) measurement respectively in the absence of measuremnt and for two measurement strength values. which label the axes All parameters are same as Fig.4.

Acknowledgments

We acknowledge several enlightening discussions with A.A. Clerk. This work is supported by the DARPA QuASAR and ORCHID programs through grants from AFOSR and ARO, the U.S. Army Research Office, and NSF. YD is supported in part by the NSFC Grants No. 11304072 and the Hangzhou-city Quantum Information and Quantum Optics Innovation Research Team. KZ is supported by the NSFC Grants No. 11204084, No. 91436211, and No. 11234003, the National Basic Research Program of China Grant No. 2011CB921604, the SRFDP Grant No. 20120076120003, and the SCST Grant No. 12ZR1443400.

Appendix A: Stochastic Schrödinger equation description of continuous measurements

This appendix outlines the main steps of derivation of a stochastic formalism that leads to the description of continuous quantum measurements in terms of stochastic master equations of stochastic Schrödinger equations. The interested reader may want to consult the excellent tutorial presentation of Ref. [47] for details.

The idea is to monitor some system observable described by a hermitian operator $\hat{X}$ during some interval divided into a large sequence of small intervals each of duration Δt. Although this is not necessary we assume for simplicity that $\hat{X}$ has a continuous spectrum of eigenvalues $\{x\}$, with eigenstates as $|x\rangle$, so that $\langle x|x'\rangle = \delta(x-x')$. Importantly, one is not in general interested in making projective measurements that would leave $\hat{X}$ in one of its eigenstates. Rather, we consider 'weaker measurements' characterized by a positive operator valued measure (POVM) $\hat{A}(\alpha)$, with

$$\hat{A}(\alpha) = \left(\frac{4k\Delta t}{\pi}\right)^{1/4} \int_{-\infty}^{+\infty} e^{-2k\Delta t(x-\alpha)^2} |x\rangle\langle x| dx, \tag{A1}$$

which provide only partial information about the observable. Each operator $\hat{A}(\alpha)$ is a Gaussian-weighted sum of projectors onto the eigenstates of $\hat{X}$. Here α is a continuous index, such that the spectrum of measurement result is a continuum labeled by α. As we shall see, the parameter k can be understood as a measure of the measurement strength. Continuous measurements result from taking the limit $\Delta t \to 0$.

In practice the measurements are realized by coupling the system to a measuring apparatus through an interaction proportional to $\hat{X}$ and a measuring device observable which is then determined by a projective measurement. In our case, the measuring apparatus is a low density beam of two-level atoms that are either resonant (absorptive case) or off-resonant (dispersive case) with the intracavity field.

For the initial state $|\psi\rangle = \int \psi(x)|x\rangle dx$, the probability distribution for obtaining the measurement outcome α is

$$\begin{aligned} P(\alpha) &= Tr[\hat{A}(\alpha)|\psi\rangle\langle\psi|\hat{A}^{\dagger}(\alpha)] \\ &= \sqrt{\frac{4k\Delta t}{\pi}} \int_{-\infty}^{+\infty} |\psi(x)|^2 e^{-4k\Delta t(\alpha-x)^2} dx, \end{aligned} \tag{A2}$$

and for Δt sufficiently small the Gaussian is much broader than $\psi(x)$, so that one can approximate $|\psi(x)|^2$ by a delta function centered at the expectation value $\langle\hat{X}\rangle$. We then have

$$P(\alpha) \simeq \sqrt{\frac{4k\Delta t}{\pi}} e^{-4k\Delta t(\alpha-\langle\hat{X}\rangle)^2}. \tag{A3}$$

It follows that we can write α as the stochastic quantity

$$\alpha = \langle\hat{X}\rangle + \frac{\Delta w}{\sqrt{8k}\Delta t} \tag{A4}$$

where Δw is a zero-mean, Gaussian random variable of variance Δt. It is the stochastic nature of α that accounts for the random nature of the quantum successive measurements. The larger k, the smaller the fluctuations in the measurement outcomes.

This permits to numerically determine the evolution of the wave function subject to measurements characterized by the POVM $\hat{A}(\alpha)$ at each time step, with the stochastic infinitesimal change of the quantum state following a single measurement given by

$$|\psi(t+\Delta t)\rangle \propto \hat{A}(\alpha)|\psi(t)\rangle \propto e^{-2k\Delta t(\alpha-\hat{X})^2}|\psi(t)\rangle. \tag{A5}$$

Expanding the exponential to first order in $\Delta t \to dt$ and to second order in the Wiener process dw (due to the Ito rule $dw^2 = dt$) and normalizing $|\psi(t+dt)\rangle$ finally gives the stochastic Schrödinger equation

$$d|\psi\rangle = [-k(\hat{X}-\langle\hat{X}\rangle)^2 dt + \sqrt{2k}(\hat{X}-\langle\hat{X}\rangle)dw]|\psi(t)\rangle. \tag{A6}$$

The explicit forms (28) and (31) result from taking $\hat{X} = (\hat{a}+\hat{a}^\dagger)$ and $\hat{X} = \hat{a}^\dagger\hat{a}$, respectively.

[1] H. E. D. Scovil and E. O. Schulz-DuBois, Phys. Rev. Lett. **2**, 262 (1959).

[2] E. Geva and R. Kosloff, J. Chem. Phys. **96**, 3054 (1992); E. Geva and R. Kosloff, J. Chem. Phys. **104**, 7681 (1996).

[3] T. Feldmann, E. Geva, R. Kosloff, and P. Salamon, Am. J. Phys. **64**, 485 (1996); T. Feldmann and R. Kosloff, Phys. Rev. E **68**, 016101 (2003).

[4] H. T. Quan, Y. X. Liu, C. P. Sun, and F. Nori, Phys. Rev. E **76**, 031105 (2007).

[5] D. Gelbwaser-Klimovsky, and G. Kurizki, Sci. Rep. **5**, 7809 (2015).

[6] F. Mazza, R. Bosisio, G. Benenti, V. Giovannetti, R. Fazio, and F. Taddei, New J. Phys. **16** 085001 (2014).

[7] J.-Q. Liao, H. Dong, and C. P. Sun, Phys. Rev. A **81**, 052121 (2010).

[8] D. Venturelli, R. Fazio, and V. Giovannetti, Phys. Rev. Lett. **110**, 256801 (2013).

[9] A. Dechant, N. Kiesel, and E. Lutz, arXiv:1408.4617;

[10] J. Roßnagel, O. Abah, F. Schmidt-Kaler, K. Singer, and E. Lutz, Phys. Rev. Lett. **112**, 030602 (2014).

[11] M. Brunelli, A. Xuereb, A. Ferraro, G. De Chiara, N. Kiesel, and M. Paternostro, arXiv:1412.4803.

[12] M. O. Scully, M. S. Zubairy, G. S. Agarwal, and H. Walther, Science **299**, 862 (2003).

[13] M. O. Scully, K. R. Chapin, K. E. Dorfman, M. B. Kim, and A. Svidzinsky, PNAS **108**, 15097 (2011).

[14] A. E. Allahverdyan and Th. M. Nieuwenhuizen, Phys. Rev. E **71**, 066102 (2005).

[15] M. Esposito and S. Mukamel, Phys. Rev. E **73**, 046129 (2006).

[16] E. Boukobza and D. J. Tannor, Phys. Rev. A **74**, 063823 (2006).

[17] P. Talkner, E. Lutz, and P. Hänggi, Phys. Rev. E **75**, 050102(R) (2007).

[18] L. Fusco, S. Pigeon, T. J. G. Apollaro, A. Xuereb, L. Mazzola, M. Campisi, A. Ferraro, M. Paternostro, and G. De Chiara, Phys. Rev. X **4**, 031029 (2014).

[19] R. Dorner, J. Goold, C. Cormick, M. Paternostro, and V. Vedral, Phys. Rev. Lett. **109**, 160601 (2012).

[20] E. Mascarenhas, H. Braganca, R. Dorner, M. Franca Santos, V. Vedral, K. Modi, J. Goold, Phys. Rev. E **89**, 062103 (2014).

[21] Tony J. G. Apollaro, Gianluca Francica, Mauro Paternostro, Michele Campisi, arXiv:1406.0648.

[22] M. Campisi, R. Blattmann, S. Kohler, D. Zueco, and P. Hänggi, New J. Phys. **15**, 105028 (2013).

[23] D. G. Joshi, and M. Campisi, Eur. Phys. J. B **86**, 157 (2013).

[24] P. Smacchia, and A. Silva, Phys. Rev. E **88**, 042109 (2013).

[25] O.-P. Saira, Y. Yoon, T. Tanttu, M. Möttönen, D. V. Averin, and J. P. Pekola, Phys. Rev. Lett. **109**, 180601(2012).

[26] T. B. Batalhão, A. M. Souza, L. Mazzola, R. Auccaise, R. S. Sarthour, I. S. Oliveira, J. Goold, G. D. Chiara, M. Paternostro, and R. M. Serra, Phys. Rev. Lett. **113**, 140601 (2014).

[27] C. Jarzynski, Nat. Phys. **11**, 105 (2015); P. Hänggi, and P. Talkner, Nature Phys. **11**, 108110 (2015); S. An, J-N. Zhang, M. Um, D. Lv, Y. Lu, J. Zhang, Z-Q. Yin, H. T. Quan, and K. Kim, Nat. Phys. **11**, 193 (2015).

[28] S. Suomela, J. Salmilehto, I. G. Savenko, T. Ala-Nissila, and M. Möttönen, Phys. Rev. E **91** 022126 (2015).

[29] J. Salmilehto, P. Solinas, and M. Möttönen, Phys. Rev. E **89** 052128 (2014).

[30] M. F. Frenzel, D. Jennings, and T. Rudolph, Phys. Rev. E **90** 052136 (2014).

[31] M. Esposito, U. Harbola and S. Mukamel, Rev. Mod. Phys. **81**, 1665(2009).

[32] M. Campisi, P. Hanggi, and P. Talkner, Rev. Mod. Phys. **83**, 771 (2011).

[33] P. Talkner, E. Lutz, and P. Hänggi, Phys. Rev. E **75**, 050102(R) (2007); P. Talkner and P. Hänggi, J. Phys. A: Math. Theor. **40**, F569 (2007). P. Talkner, P. Hänggi, and M. Morillo, Phys. Rev. E **77**, 051131 (2008); M. Campisi, P. Talkner, and P. Hänggi, Philos. Trans. R. Soc. A **369**, 291 (2011).

[34] S. Mukamel, Phys. Rev. Lett. **90**, 170604 (2003).

[35] A. J. Roncaglia, F. Cerisola, and J. P. Paz, Phys.Rev.Lett.**113**, 250601(2014); G. D. Chiara, A. J Roncaglia, and J. P. Paz, New J. Phys. **17**, 035004 (2015).

[36] G. E. Crooks, J. Stat. Mech.: Theor. Exp. (2008) P10023.

[37] M. Campisi, P. Talkner, and P. Hänggi, Phys. Rev. Lett. **102**, 210401 (2009); P. Talkner, M. Campisi, and P. Hänggi, J. Stat. Mech.: Theor. Exp. (2009) P02025; M. Campisi, P. Talkner, and P. Hänggi, Phys. Rev. Lett. **105**, 140601 (2010).

[38] F. Ritort, Physics 2, 43 (2009).

[39] See e.g. J. M. Horowitz, Phys Rev E. **85** 031110 (2012) and references therein.

[40] M. Esposito, U. Harbola, and S. Mukamel, Phys. Rev. E **76**, 031132 (2007); M. Esposito and C. Van den Broeck, Phys. Rev. Lett. **104**, 090601 (2010).

[41] U. Seifert, Phys. Rev. Lett. **95**, 040602 (2005); T. Schmiedl, T. Speck, and U. Seifert, J. Stat. Phys. **128**, 77 (2007);T. Schmiedl and U. Seifert, J. Chem. Phys. **126**, 044101 (2007); U. Seifert, Eur. Phys. J. B **64**, 423 (2008).

[42] M. Aspelmeyer, T. Kippenberg and F. Marquardt, Rev. Mod. Phys. **86**, 1391 (2014); P. Meystre, Ann. Phys. (Berlin) **525**, 215 (2013).

[43] K. Zhang, F. Bariani, and P. Meystre, Phys. Rev. Lett. **112**, 150602 (2014); K. Zhang, F. Bariani, and P. Meystre, Phys. Rev. A **90**, 023819 (2014) and references therein.

[44] M. Paternostro, S. Gigan, M. S. Kim, F. Blaser, H. R. Böhm, and M. Aspelmeyer, New Journal of Physics **8**, 107 (2006); I. Wilson-Rae, N. Nooshi, J. Dobrindt, T. J. Kippenberg, and W. Zwerger, New J. Phys. **10**, 095007 (2008).

[45] In quantum Otto cycles the isochoric strokes of classical heat engines are replaced by thermalization processes at fixed detunings, see Ref. [4] for a clear discussion of this point.

[46] T. D. Kieu, Phys. Rev. Lett. **93**, 140403 (2004); J. Gemmer, M. Michel, and G. Mahler, *Quantum Thermodynamics* (Springer, Berlin, Germany 2010).

[47] K. Jacobs and D. A. Steck, Contemporary Physics, **47**, 279 (2006).

[48] H. Carmichael, *An Open Quantum Systems Approach to Quantum Optics* (Springer, Berlin, 1993).

[49] H. M. Wiseman, Ph.D. thesis, University of Queensland (1994).

[50] M. Plenio and P. L.Knight, Rev. Mod. Phys. **70**, 101 (1998).

[51] N. Imoto, Masahito Ueda, and Tetsuo Ogawa, Phys. Rev. A **41**, 4127 (1990).

[52] M. Ueda, Nobuyuki Imoto, H. Nagaoka, and T. Ogawa, Phys. Rev. A **46**, 2859 (1992).

[53] P. Solinas, D. V. Averin, and J. P. Pekola, Phys. Rev. B **87**, 060508(R) (2013).

[54] Remember that in the thermodynamic convention work performed by the engine is negative.

[55] Y. Dong. F. Bariani and P. Meystre, arXiv:1507.07337 .